

Probing water compartments and membrane permeability in plant cells by ^1H NMR relaxation measurements

J. E. M. Snaar and H. Van As

Department of Molecular Physics, Agricultural University, 6703 HA Wageningen, The Netherlands

ABSTRACT ^1H NMR relaxation times (T_1 and T_2) in parenchyma tissue of apple can identify three populations of water with different relaxation characteristics. By following the uptake of Mn^{2+} ions in the tissue it is shown that the observed relaxation times originate from particular water compartments: the vacuole, the cytoplasm, and the cell wall/extracellular space.

Proton exchange between these compartments is controlled by the plasmalemma and tonoplast membranes. During the Mn^{2+} penetration experiment, conditions occur that cause the relaxation times of protons of cytoplasmic water to be much shorter than their residence time in the cytoplasm. Then the tonoplast permeability coefficient P_d for water can be calculated from the vacuolar T_1 and T_2 values to be $2.44 \cdot 10^{-6} \text{ m} \cdot \text{s}^{-1}$.

INTRODUCTION

NMR relaxation time measurements have been widely used to investigate the physical properties of water in various plant tissues (1, 2). The ^1H NMR spin-lattice (T_1) and spin-spin (T_2) relaxation times of water are related to the water content of the plant tissue, the properties of water in different parts of the tissue, and interactions with macromolecules (1, 3–5). T_1 and/or T_2 have been used to describe the plant water status (6–8). Within plant cells different water compartments can be discriminated. Between these compartments water molecules or protons are in exchange, resulting in averaging of the intrinsic relaxation times and the observed relative amplitudes of water in these compartments, preventing the direct assignment of relaxation times to particular compartments. The amount of averaging depends on the exchange rates, the intrinsic relaxation times, and the cell morphology. The exchange rates between the compartments are controlled by the (proton) permeability of the membranes separating the compartments and/or by the diffusion process by which water molecules reach the membranes.

Generally, ^1H relaxation of water in plant tissue is multiexponential and much faster than that of bulk water. Multiexponential decay has been suggested previously to reflect water in different plant cell compartments (4, 5, 9). If correct, this would be very valuable for the study of the sub cellular water distribution of plant tissue and for the understanding of the transport properties of water molecules in sub cellular compartments. Multiexponential decay curves must be interpreted with caution, however, since multiexponential relaxation can have several different causes: cellular heterogeneity, sub-cellular compartmentation (1, 10), and even the presence of relaxation sinks at the boundaries of homogeneous compartments (3). In addition, even the most advanced analysis of multiexponential decay requires high

quality decay curves to be able to reliably resolve several (typically up to four) components.

Here, we report the results of a detailed study of proton relaxation of water in parenchyma storage tissue of apple fruit, as affected by the penetration of paramagnetic Mn^{2+} ions into the tissue via extracellular spaces. The Mn^{2+} ions penetrate successively into the extracellular space, cytoplasm, and vacuole. The paramagnetic ions enhance the proton relaxation rates of water in contact with these ions. The combination of accurate relaxation time measurements, T_2 , T_1 , and T_2 -weighted T_1 (10), and the Mn^{2+} penetration process can be used to assign particular proton relaxation components to water in particular cell compartments.

MATERIALS AND METHODS

NMR measurements

The experiments were carried out using a 20-MHz single-coil pulsed ^1H NMR spectrometer (11). T_2 was measured using a modified Carr-Purcell-Meiboom-Gill (CPMG) pulse sequence (12). T_1 was measured using a saturation recovery (SR) sequence and T_2 -weighted T_1 using a SR-CPMG sequence (10). This latter sequence allows the simultaneous determination of (SR) T_1 and (CPMG) T_2 values and in addition T_2 -weighted T_1 values by plotting the analyzed T_2 amplitudes as functions of the recovery time, resulting in correlated observed T_2 and T_1 values in compartmentalized systems. Experimental details are as reported elsewhere (10).

Plant material

Apple parenchyma tissue (Cox, var) was chosen because of its relatively uniform cell size and low metabolic activity, which is constant for several hours. Small samples were taken from the inner part of the fruit ($\pm 25 \text{ mm}^3$) and measured directly or after exposure to a 50-mM MnCl_2 -200-mM mannitol solution. The NMR sample tubes were sealed during measurements. The cells in this part of the fruit had an average cell diameter of $\pm 132 \mu\text{m}$, and are approximately spherical.

Different samples from the same fruit were immersed in the solution for various times (from a few minutes to 22 h). Just before the T_1 and T_2 -weighted T_1 measurements, a sample was taken out of the solution and blotted with paper to remove excess liquid. The remaining film of Mn^{2+} solution covering the apple tissue did not interfere with the measurement of the intracellular water ^1H relaxation. Different samples

Address correspondence to Dr. H. Van As, Department of Molecular Physics, Agricultural University, Dreijenlaan 3, 6703 HA Wageningen, The Netherlands.

TABLE 1 T_2 and T_2 -weighted T_1 values and their relative amplitudes P of untreated apple tissue measured using the CPMG and SR-CPMG sequence

Fraction	T_2	T_2 -weighted T_1	P
	s	s	%
a	1.02	1.37	75.2
b	0.19	0.68	16.4
c	0.03	0.35	8.4

were used to study the time-dependent effect of Mn^{2+} penetration on the values of the T_1 and the T_2 -weighted T_1 . T_2 measurements could be performed in the presence of the solution in view of the short time required for a T_2 measurement. The uptake of Mn^{2+} was followed for one particular piece of apple tissue in the course of time.

RESULTS AND DISCUSSION

Initial observations

T_2 -weighted T_1 and T_2 relaxation time measurements of fresh tissue, not treated with Mn^{2+} solution, yield decay curves that were found to be optimally described by three exponentials (Table 1). One fraction, labeled P_a , has a relative amplitude of 75.2% of the total water signal, and has the longest T_2 and T_2 -weighted T_1 times. The second fraction (P_b) represents 16.4%, whereas the third fraction (P_c) represents the remaining 8.4% of the water signal, and has the shortest relaxation times. T_2 measurements on 13 different samples revealed a standard deviation of 4% for T_{2a} , 9% for T_{2b} , and 9% for T_{2c} . By contrast with T_2 and T_2 -weighted T_1 results, T_1 measurements resulted in the observation of two exponentials. The fraction with the longer T_1 represents 80% and that with the shorter T_1 20% of the water signal.

On the origin of fractions

The effect of paramagnetic ions on the relaxation times of the three fractions depends on the period, during which the tissue has been immersed in the solution. Fig. 1 *A* and *B* show the $1/T_2$ values of the three observed fractions and the corresponding amplitudes, respectively, of water in apple tissue exposed to a Mn^{2+} /mannitol solution versus the penetration period. All curves are normalized to their initial values $1/T_2^0$, defined as the initial values of $1/T_{2a}$, $1/T_{2b}$, and $1/T_{2c}$ respectively, of the fresh tissue before the start of the penetration, and thus coincide at $t = 0$ at the value of 1 for each curve (the horizontal dashed line at the value of $T_2^0/T_2 = 1$ is given for reference). The amplitudes and T_2^0/T_2 values were plotted versus the square root of time because this enables a contraction of the long time scale and it was expected that the Mn^{2+} penetration resembles a diffusion process. The curve of Fig. 1 *A* can be divided into three regions, I, II, and III, for T_{2a} and T_{2b} , and two regions for T_{2c} . Fig. 1 *B* shows that the Mn^{2+} /mannitol solution does not introduce dramatic changes in the water bal-

ance. Since a 50-mM Mn^{2+} solution is hypotonic for apple tissue, mannitol has been added while mannitol acts as an osmoticum and prevents the distortions of the water balance. T_1 decays, although biexponential, resulted in penetration curves that could also be divided into three regions for each separate T_1 value (results not shown). A similar three-phase pattern during Mn^{2+} uptake has also been observed for water in maize roots based on a single intracellular T_1 value (4). When the

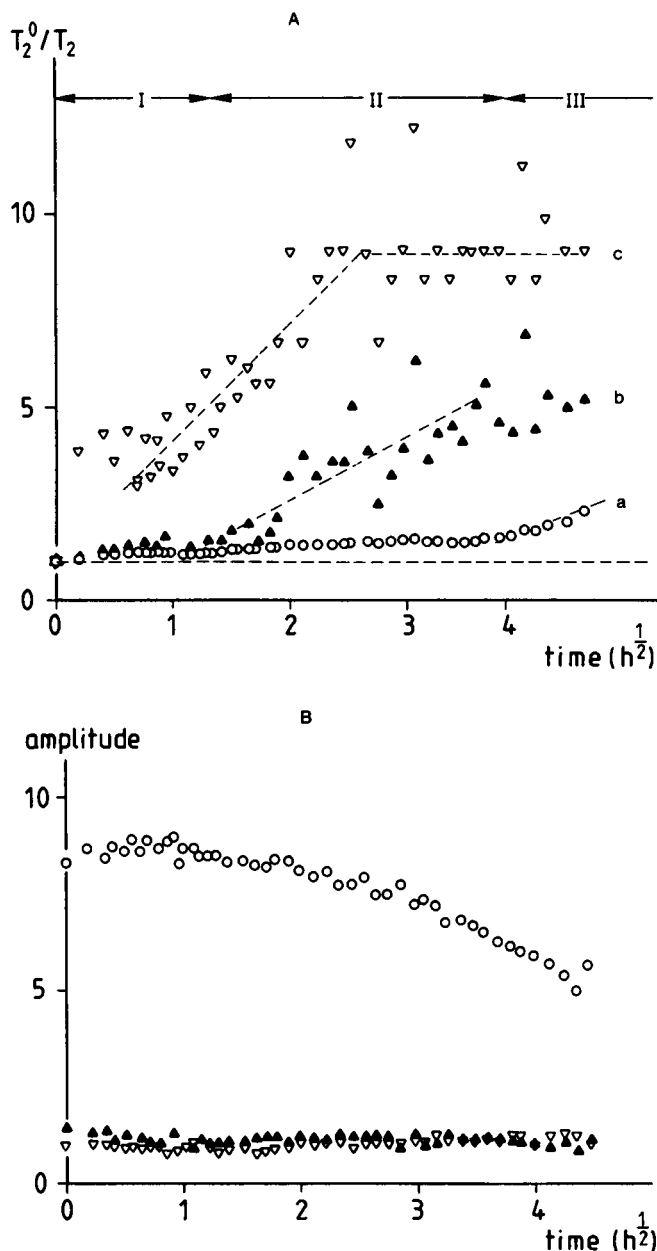


FIGURE 1 The effect of penetration of Mn^{2+} ions in time on the proton relaxation of water in apple tissue: (A) normalized relaxation rates T_2^0/T_2 ; (a) (\circ) T_{2a} ; (b) (\blacktriangle) T_{2b} ; (c) (∇) T_{2c} . (B) the amplitudes of the fractions corresponding to the three relaxation rates. The NMR measurements were carried out in the presence of a 50-mM Mn^{2+} -200-mM mannitol solution. The fast decaying component of this solution with a T_2 value of 0.5 ms is not shown here.

penetration experiment starts with tissue that has been vacuum-infiltrated with the Mn^{2+} /mannitol solution before being exposed to that solution, a two-phase absorption curve is observed for T_{2a} and T_{2b} , and a single phase for T_{2c} (Fig. 2). Comparison of Fig. 1 A and 2 shows that phase I in Fig. 1 A is absent in Fig. 2, evidently as a result of vacuum-infiltration.

$1/T_{2c}$ in Fig. 1 A initially increases during the time that is required for Mn^{2+} to reach the cell wall by diffusion through the extracellular space and becomes constant during phase II. T_{2c} can be ascribed to water in the extracellular space and cell wall. The steady state value is reached at $t = 0$ in Fig. 2 because now the cell wall/extracellular space is immediately filled due to vacuum-infiltration. The T_2 values found for cell walls depend on the water content, e.g., for ivy bark a value of 5–10 ms was found (9) and apple cell wall preparation, rehydrated up to 85% by weight of water, yielded a value of 30 ms (5). Our T_{2c} value of untreated apple tissue of ± 30 ms corresponds with these values. During period I (Fig. 1 A), $1/T_{2b}$ and $1/T_{2a}$ also show an initial increase, but to a much lesser extent than $1/T_{2c}$, and become constant long before $1/T_{2c}$ has reached its steady-state value. If there is exchange of protons over the plasmalemma, an increase of the $1/T_2$ value of water in the extracellular space/cell wall results in an increase of $1/T_2$ of water in the cell.

After the initial loading period of ± 2.75 h a gradual change in the $1/T_{2b}$ over several hours was observed (Fig. 1 A phase II) as is also observed for $1/T_{2b}$ in the first part of Fig. 2. This second phase represents the in-

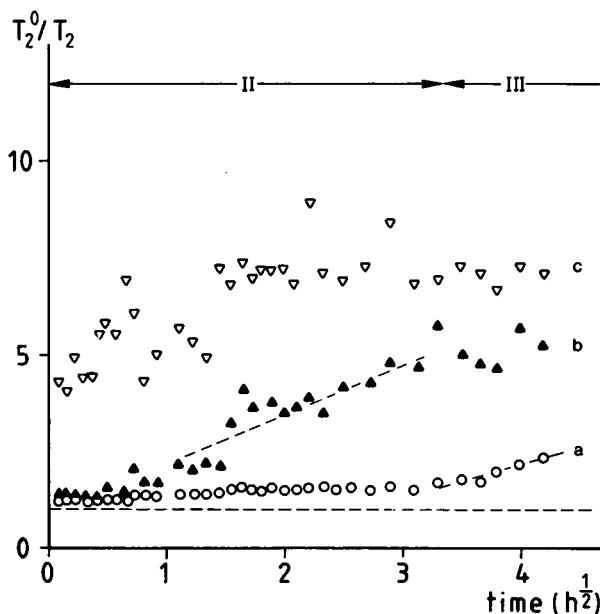
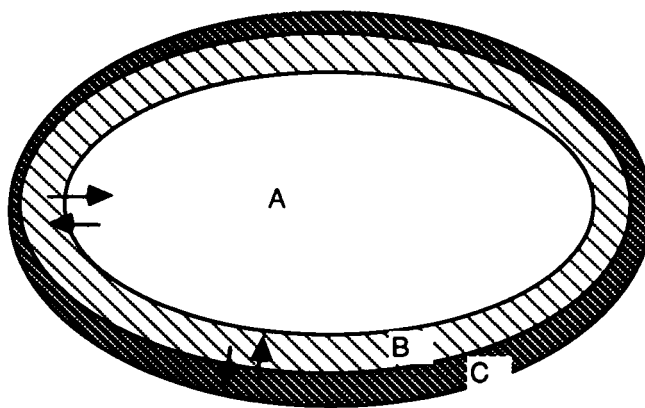


FIGURE 2 Dependence of the normalized relaxation rates T_2^0/T_2 of water protons of apple tissue on the penetration of Mn^{2+} ions, after vacuum-infiltration with the solution before the measurement. Further details: see legend of Fig. 1.



A: vacuole
B: cytoplasm
C: cell wall/extracellular space

FIGURE 3 A model to explain relaxation measurements in vacuolated plant tissue. Water in the vacuole, cytoplasm, and cell wall/extracellular space can be discriminated. Within these compartments diffusional averaging results in single exponential relaxation behavior. Proton exchange across the plasmalemma and the tonoplast membranes results in a further averaging of the intrinsic relaxation times of water in these compartments.

flux of Mn^{2+} into the cytoplasm, and indicates that T_{2b} corresponds to cytoplasmic water. Region III, after ± 16 h, represents the influx of Mn^{2+} into the vacuole, T_{2a} corresponding to vacuolar water. Water in the vacuole is expected to have the longest relaxation times and the largest fraction, as is observed at $t = 0$ (see Table 1).

Water heterogeneity within the three compartments mentioned above results in single exponential relaxation decay due to diffusive exchange (13). The vacuole is much larger than the range of sizes suggested for the observation of multiexponential relaxation within one homogeneous compartment (3), therefore vacuolar water can only give rise to a single relaxation time. Diffusive exchange between the compartments, averaging the proton magnetization, is slowed down by the plasmalemma and tonoplast. These arguments support the idea that the observed relaxation times, one by one, correspond to the three above-mentioned compartments. Exchange of water protons over the tonoplast and plasmalemma is reflected in the measured values of P_a , P_b , P_c , and $T_{1,2a}$, $T_{1,2b}$, $T_{1,2c}$, since the observed values depend on the ratio between the exchange rates and the relaxation rates. The above mentioned results are interpreted using a model presented in Fig. 3.

The effect of exchange between the compartments with respect to the relaxation rates within the compartments is evident in the results of the manganese penetration experiment. After an initial increase $1/T_{2a}$ becomes constant again during phase II (Figs. 1 A and 2) and most likely occurs as soon as the relaxation rate of water in the cytoplasm becomes faster than the exchange rate

TABLE 2 T_2 and T_2 -weighted T_1 values of apple tissue measured after exposure to a Mn^{2+} /mannitol solution during 6 h

Fraction	T_2	T_2 -weighted T_1
	s	s
a	0.66	0.66
b	0.038	0.08
c	0.003	0.02

over the tonoplast. When this condition is fulfilled, the relaxation rates of water in the vacuole become a function of the intrinsic relaxation rates of vacuolar water and the proton exchange rate between vacuole and cytoplasm (14). Since vacuolar water at this field strength is expected to have equal intrinsic T_1^i and T_2^i values (1) the observed relaxation times of vacuolar water are then solely determined by the exchange rate over the tonoplast, which equally affects T_1 and T_2 . Therefore, the observed T_1 and T_2 of vacuolar water become equal if the relaxation rate in the cytoplasm is much shorter than the exchange rate. This is verified by T_2 -weighted T_1 values measured after exposing the tissue to the Mn^{2+} solution during a period of 6 h (Table 2). Whereas at $t = 0$ T_2 -weighted T_{1a} is longer than T_{2a} , their values become equal during the period 4–16 h (Fig. 1 A).

T_1 measurements reveal the same three-phase pattern, the shortest and the longest T_1 decreasing continuously during Mn^{2+} penetration, but at different rates (results not shown). Although the effect of exchange over the tonoplast affects T_1 , the effect of Mn^{2+} penetration on T_1 is less than on T_2 . This can be explained when the backflux of magnetization from cytoplasm to vacuole cannot be neglected with respect to T_1 relaxation before the influx of Mn^{2+} into the vacuole becomes manifest. Then a continuous decrease of T_1 values is observed.

Calculation of the proton permeability coefficient of the tonoplast

The mean residence time t_a for water in the vacuole can be calculated from the observed T_{2a} or T_2 -weighted T_{1a} during the period of 4–16 h (Fig. 1 A), using the Conlon–Outhred technique (14). If backflux of magnetization from cytoplasm to vacuole can be neglected by making $1/T_b$ very large, the observed vacuolar relaxation rate, $1/T_a$, is given by

$$1/T_a = 1/T_a^i + 1/t_a \quad (1)$$

where $1/T_a^i$ is the intrinsic relaxation rate of the vacuole. The initial observed T_2 -weighted T_{1a} and T_{2a} , in the absence of Mn^{2+} , do not equal the intrinsic relaxation times of the vacuole, but are also affected by exchange between vacuole and cytoplasm. The vacuolar sap is a relatively dilute solution of ions and vacuolar water and can be considered as bulk water with $T_2^i = T_1^i \approx 2.4$ s. Therefore, T_1 should be equal to T_2 , which is indeed

observed for the plateau in region II, with observed values T_2 -weighted $T_1 = T_2 = 0.66$ s. From Eq. 1, t_a can now be calculated and was found to be 0.9 s. When t_a is controlled by the membrane permeability and not by rate-limiting diffusion the proton permeability coefficient P_d of the tonoplast can be calculated. This condition is fulfilled, assuming a spherical geometry for the vacuole, if $3Dt_a/r^2 > 1$. We determined from NMR diffusion measurements for apple tissue $r = 66 \mu\text{m}$ and $D = 2.2 \cdot 10^{-9} \text{ m}^2 \text{ s}^{-1}$ (Snaar, J. E. M., and H. Van As, unpublished results) yielding $3Dt_a/r^2 = 1.36$. The tonoplast permeability is therefore rate-limiting. The P_d can be calculated using

$$P_d = V/(At_a) = r/(3t_a) \quad (2)$$

A value for P_d of $2.44 \cdot 10^{-5} \text{ m s}^{-1}$ is calculated for the tonoplast.

Published water permeability measurements for plants indicate a wide range of values. Values differing by a factor of 10 or more have been measured with NMR e.g., the P_d for ivy bark was estimated to be $3 \cdot 10^{-4} \text{ m} \cdot \text{s}^{-1}$ (9), for *Nitella* cells a value of $2.5 \cdot 10^{-5} \text{ m} \cdot \text{s}^{-1}$ has been reported (15). A mutual comparison cannot simply be made, nor can it be assumed that the widely different P_d values represent a difference between species, due to variation in membrane permeability, since the methods by which the values are obtained are different. For example, the relaxation time found for a sample without paramagnetic ions has been used as the intrinsic T_1 or T_2 (4), and the P_d obtained from a two-component solution (9) may represent the tonoplast P_d or an averaged tonoplast/plasmalemma P_d on the other hand.

General remarks

Up to now the interpretation of relaxation data, T_1 or T_2 , has been based on analysis of decay curves into, at the most, two exponentials. The long relaxation times are ascribed to intracellular bulk water, and the short times to cell wall and extracellular bulk water. Water in the cytoplasm has either been included in the intracellular fraction (9) or has been associated with the membranes and cell wall (4, 5). By contrast, we found two T_1 and three T_2 -weighted T_1 and T_2 relaxation times as a result of our improved method (10) to measure these relaxation times. Differences between fast or intermediate/slow exchange between vacuole and cytoplasm with respect to T_1 and T_2 relaxation, respectively, can explain the different number of exponentials found for T_1 or T_2 . Whereas the T_2 -weighted T_1 times reflect T_1 - and T_2 -exchange kinetics (10), again three T_2 -weighted T_1 values are observed. The difference between T_1 - and T_2 -exchange kinetics also explains the different time dependence of T_1 and T_2 for apple tissue exposed to Mn^{2+} : the T_2 results show different patterns for each T_2 component, in contrast to the T_1 results. This difference does not necessarily hold for all types of plant tissue. Gener-

ally, accurate T_2 measurements yield more detailed information on the partitioning of water in subcellular compartments in plant tissue than T_1 measurements. The combination of measurements of different relaxation times gives not only insight in the origin of fractions but also on the transport properties of water.

The authors wish to thank Professor Dr. T. J. Schaafsma for stimulating discussions and critical reading of the manuscript.

Received for publication 16 June 1992 and in final form 25 August 1992.

REFERENCES

1. Belton, P. S., and R. G. Ratcliffe. 1985. NMR and compartmentation in biological tissues. *Prog. NMR Spectroscopy*. 17:241–279.
2. Connelly, A., J. A. B. Lohman, B. C. Loughman, H. Quiquampoix, and R. G. Ratcliffe. 1987. High resolution imaging of plant tissue by NMR. *J. Exp. Botany*. 38:1713–1723.
3. Brownstein, K. R., and C. E. Tarr. 1979. Importance of classical diffusion in NMR studies of water in biological cells. *Phys. Rev. A*. 19(6):2446–2453.
4. Bačić, G., and S. Ratković. 1984. Water exchange in plant tissue studied by proton NMR in the presence of paramagnetic centers. *Biophys. J.* 45:767–776.
5. Hills, B. P., and S. L. Duce. 1990. The influence of chemical and diffusive exchange on the water proton transverse relaxation in plant tissues. *Magn. Reson. Imaging*. 8:321–331.
6. Colire, C., E. Le Rumeur, J. Gallier, J. de Certaines, and F. Larher. 1988. An assessment of proton magnetic resonance as an alternative method to describe water status of leaf tissues in wilted plants. *Plant Physiol. Biochem.* 26:767–776.
7. Van As, H., T. J. Schaafsma, and J. Blaakmeer. 1986. Applications of NMR to water flow and balance in plants. *Acta Hort.* 174:491–495.
8. Reinders, J. E. A., H. Van As, T. J. Schaafsma, P. A. de Jager, and D. W. Sherrif. 1988. Water balance in *Cucumis* plants, measured by NMR. *J. Exp. Bot.* 39:1199–1210.
9. Stout, D. G., P. L. Steponkus, and R. M. Cotts. 1978. Nuclear magnetic resonance relaxation times and plasmalemma water exchange in Ivy Bark. *Plant Physiol.* 62:636–641.
10. Snaar, J. E. M., and H. Van As. 1992. A method for the simultaneous measurement of NMR spin-lattice and spin-spin relaxation times in compartmentalized systems. *J. Magn. Reson.* 98:139–148.
11. Van As, H., A. A. M. Brouwers, and J. E. M. Snaar. 1985. Localized real time blood flow measurements. *Arch. Int. Physiol. Biochem.* 93(5):87–96.
12. Van As, H., W. P. A. van Vliet, and T. J. Schaafsma. 1980. ^1H spin-echo nuclear magnetic resonance in plant tissue, I. the effect of Mn(II) and water content in wheat leaves. *Biophys. J.* 32:1043–1050.
13. Belton, P. S., and B. P. Hills. 1987. The effects of diffusive exchange in heterogeneous systems on NMR line shapes and relaxation processes. *Molec. Phys.* 61(4):999–1018.
14. Conlon, T., and R. Outhred. 1972. Water diffusion permeability of erythrocytes using a nuclear magnetic resonance technique. *Biochim. Biophys. Acta*. 288:354–361.
15. Ratković, S., and G. Bačić. 1980. Water exchange in *Nitella* cells: A PMR study in the presence of paramagnetic Mn^{2+} ions. *Bioelectrochem. Bioenerg.* 7:405–412.